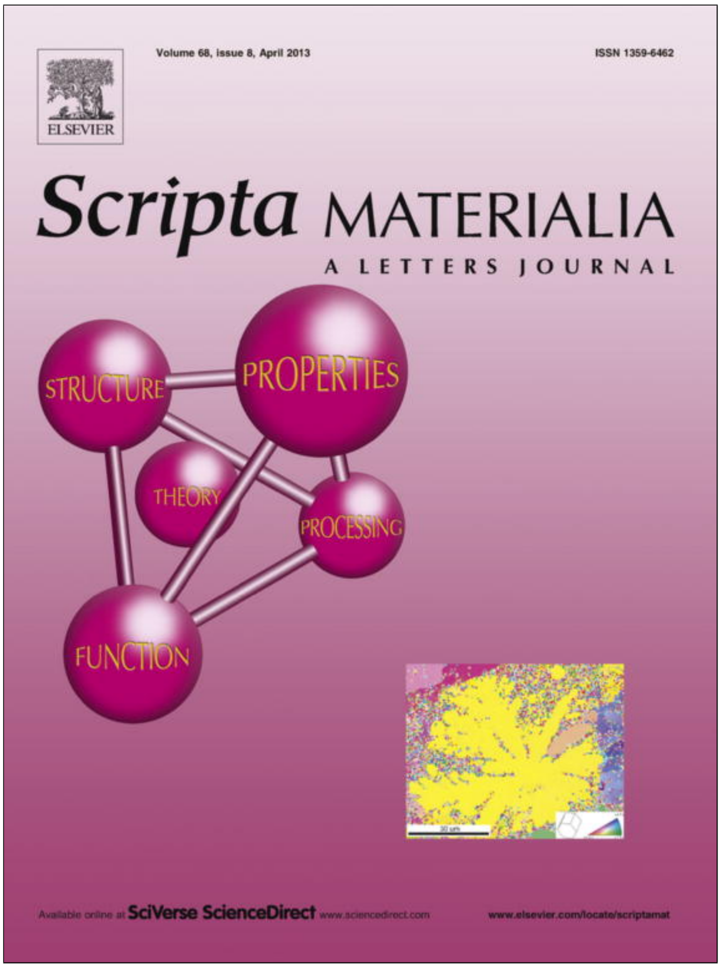
Volume 68, issue 8, April 2013
ISSN 1359-6462
ELSEVIER
Scripta MATERIALIA
A LETTERS JOURNAL
STRUCTURE
PROPERTIES
THEORY
PROCESSING
FUNCTION
Available online at SciVerse ScienceDirect www.sciencedirect.com
www.elsevier.com/locate/scriptamat

Available online at www.sciencedirect.com

SciVerse ScienceDirect

Scripta Materialia 68 (2013) 631–634

Scripta MATERIALIA

www.elsevier.com/locate/scriptamat

Formation of micro shear bands during cyclic deformation of sub-microcrystalline nickel

Suhash R. Dey,[a,*] L. Hollang,[b] B. Beausir,[c] E. Hieckmann[d] and W. Skrotzki[b]

[a]*Department of Materials Science and Engineering, Indian Institute of Technology, Hyderabad, Yeddumailaram 502205, India*
[b]*Institut für Strukturphysik, Technische Universität Dresden, 01062 Dresden, Germany*
[c]*Laboratoire d'Etude des Microstructures et de Mécanique des Matériaux (LEM3), Université Paul-Verlaine de Metz, 57012 Metz, France*
[d]*Institut für Angewandte Physik, Technische Universität Dresden, 01062 Dresden, Germany*

Received 4 September 2012; revised 22 November 2012; accepted 18 December 2012
Available online 28 December 2012

Cyclic deformation of sub-microcrystalline nickel at high plastic strain amplitude generated macro shear bands, causing fatal cracking. The macro shear bands consisted of several micro shear bands, each band containing a single layer of elliptical grains that appeared at less than 50° with respect to the loading axis. Micro texture investigations in micro shear bands revealed almost the same texture with similar shear values as in macro shear bands. During cyclic deformation local overlapping of evolving micro shear bands resulted in formation of fatal macro shear bands.

Keywords: Sub-microcrystalline nickel; Cyclic deformation; Electron backscatter diffraction; Shear band

Decreasing the grain size of polycrystalline materials to the sub-micrometer region is potentially beneficial for structural applications, in particular due to the increase in strength (e.g. [1]). Unfortunately, when cyclically deformed, sub-microcrystalline, and even more so nanocrystalline, materials exhibit a tendency to microstructural instability due to grain coarsening [2–4] sometimes accompanied by shear banding [5–8]. In a previous paper [9] the authors investigated the cyclic behaviour of sub-microcrystalline nickel (160 nm grain size produced by pulsed electrodeposition) at high plastic strain amplitude $\varepsilon_{pa} = 10^{-2}$ at room temperature. The authors reported the occurrence of pronounced homogeneous softening which was suddenly terminated by localized deformation in a macro shear band (tens of d thick) appearing under 45° that cracked very quickly. Traces of the instabilities could be seen very clearly in the microstructure: homogeneous grain coarsening without texture evolution on the one hand, and a macro shear band exhibiting strongly elongated grains with a very pronounced simple shear texture on the other. However, Ref. [9] left open the question: what is the microstructural mechanism leading to the observed sudden transition from homogeneous cyclic softening to localized macro shear banding?

Hence, the present work deals with further in-depth investigation of the microstructure and texture surrounding the macro shear band. As in Ref. [9] the data were obtained using electron backscatter diffraction (EBSD) in a Zeiss Ultra 55 scanning electron microscope equipped with a field emission gun. Processing and analysis of the acquired EBSD data were done using EBSDmcf© software developed by one of the co-authors [10].

The sheared specimen was first mechanically ground until the cracked tip surface was exposed (after ~2.3 mm) and finally electropolished. An EBSD mapping of size $89 \times 35\ \mu m^2$ was taken on this surface in the vicinity of the macro shear band covering area (c) in Figure 2a of Ref. [9]. The resulting orientation image map (inverse pole figure image with colours representing crystallographic directions parallel to the growth direction of the specimen) is shown in Figure 1a. Several grains elongated in a particular direction can be seen. Ideally, a circular-shaped grain after a certain shear γ becomes elliptical (where a is the long axis and b is the small axis of the ellipse) and the ellipse is inclined at an angle α with respect to the shear direction. The

* Corresponding author. Tel.: +91 4023016096; fax: +91 4023016032; e-mail: suhash@iith.ac.in

1359-6462/$ - see front matter © 2012 Acta Materialia Inc. Published by Elsevier Ltd. All rights reserved.
http://dx.doi.org/10.1016/j.scriptamat.2012.12.023

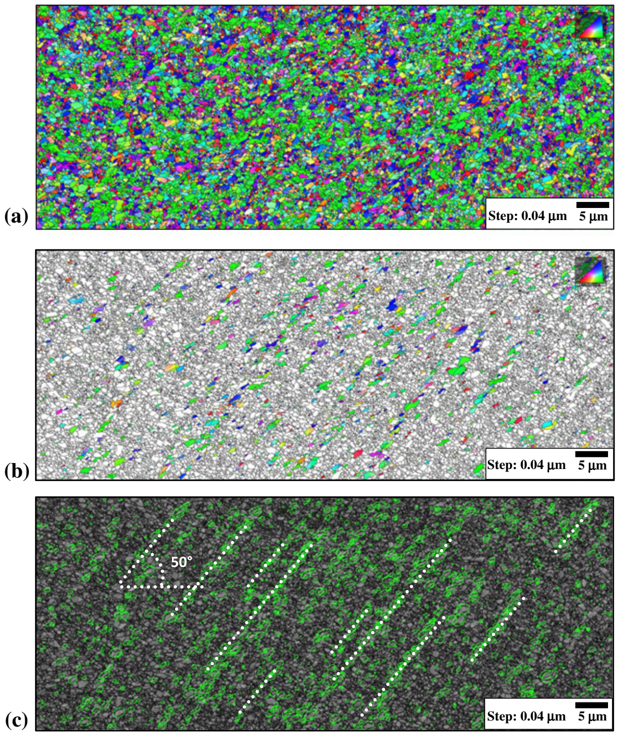

Figure 1. (a) Inverse pole figure image with the grain colours representing the crystallographic direction parallel to the growth direction of the electrodeposited specimen. (b) Coloured grains display an ellipticity of >0.5 and an inclination angle α of between 15° and 45°. (c) Elliptical fit in the selected range superimposed on the so-called "band contrast", grains arranged in micro shear bands inclined by 50° with respect to the LA.

relations between inclination angle, shape of the ellipse and amount of shear are as follows [11]:

$$\alpha = \frac{1}{2} arctg\left(\frac{2}{\gamma}\right) \tag{1}$$

$$\frac{a}{b} = \frac{1}{2}(\gamma^2 + 2 + \gamma\sqrt{\gamma^2 + 4}) = \frac{1}{1-e}, \tag{2}$$

where e is the "ellipticity". Note that α is initially 45° and tends to 0° when γ increases. Conversely, $e = 1 - b/a = 0$ in the case of a circular grain and tends to 1 with increasing γ. In Figure 1b all grains having values $0.5 < e < 1$ and $15° < \alpha < 45°$ are selected from the orientation map and remain coloured. Interestingly, the grains thus obtained are not randomly distributed in the map but are arranged in single strings under 50° with respect to the loading axis (LA). In reality, the strings of grains in the map are traces of only one system of layer-like micro shear bands of thickness d extended perpendicular to the map plane. The average grain size in the micro shear band is found to be 390 nm, the rest of the grains are 248 nm while the overall average grain size in the map is 255 nm. In Ref. [9] the grain size in the "deformed area" far away from the crack was reported to be 190 and 240 nm in the macro shear band.

The micro shear bands are separated by about 5–10 µm. It is interesting to note that the sheared grains in these micro shear bands are placed along a line that 50° to the LA—and not 45°. It is well known that in metallic glasses deformation and fracture do not occur along the planes of maximum shear stress (i.e. under 45° with respect to the LA), but under 54° in tension and under 43° in compression [12]. The reason for this is the influence of the normal stress on the deformation process. Nevertheless, in the case of the cyclically deformed sub-microcrystalline nickel discussed here the macro shear band that finally cracked appeared at exactly 45° with respect to LA (cf. Fig. 2b in Ref. [9]). Perhaps, the cooperative shear of several grains is energetically favourable along the 45° direction while the sheared grains arrange themselves along lines of 50°.

The fractions of grains (i.e. all grains, the sheared grains and the rest) with respect to their ellipticity values e are calculated and are given in Figure 2a. The fraction of sheared grains in the shear bands displays an average ellipticity of 0.6, leading to a shear value $\gamma \approx 1$. Note that it is not always possible to rely on e values to calculate γ since metal/alloy grains formed under severe shear, and therefore having e close to 1, usually fragment into several smaller grains [13]. This can in fact be observed in Figure 2b where fragmentation led to a decrease in the ellipticity shear value while the shear value calculated from the inclination angle remains the same with more points (depending upon the number of fragments) in the graph. Hence, an average shear value of 1.0 is considered and it is assumed that not many grains are affected by fragmentation.

The textures of the complete orientation map, the micro shear bands and the rest are given in Figure 3a. These textures are shear textures which have been simu-

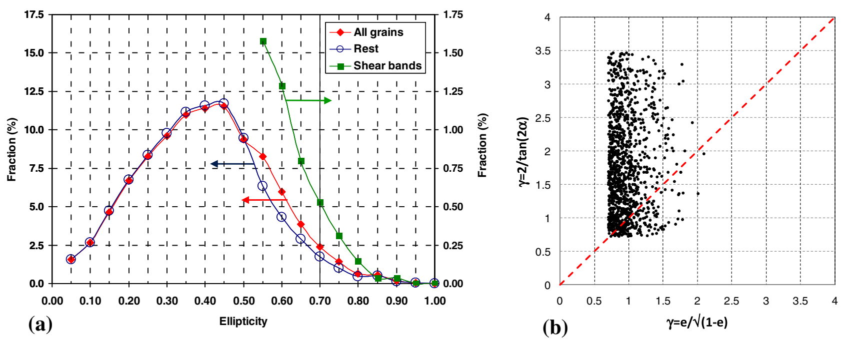

Figure 2. (a) Ellipticity of all grains (full red diamonds, left scale), sheared grains (full green squares, right scale) in the micro shear bands and the rest (open blue circles, left scale). (b) Shear strain calculated from the measured ellipticity as a function of shear strain calculated from the measured inclination angle. (For interpretation of the references to colour in this figure legend, the reader is referred to the web version of this article.)

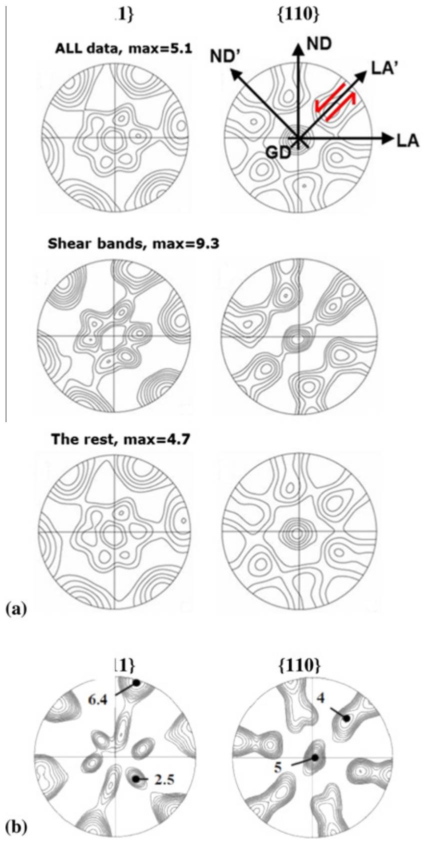

Figure 3. (a) {111} and {110} pole figures of the entire orientation map, the sheared grains and the rest of grains. Also shown is the shear plane with normal ND' which is inclined at 45° with respect to the LA. LA is the shear direction, GD is the growth direction. (b) Simulated texture based on experimentally determined values of $\gamma = 1.0$ and $m = 0.1$. Isoline values are: 0.8, 1.0, 1.3, 1.6, 2.0, 2.5, 3.2, 4.0, 5.0, 6.4.

lated previously with the viscoplastic self-consistent (VPSC) polycrystal texture model by applying shear on $\{111\}\langle 110\rangle$ slip systems [9]. The strength of shear texture in the micro shear bands is about twice that in the region in between, thus indicating strain localization into micro shear bands, maintaining a certain inter-band distance during cyclic deformation. Applying the experimentally estimated shear of $\gamma \approx 1.0$ with a strain rate sensitivity m of 0.1 in the plane at 45° with respect to the LA, the VPSC model reproduces the texture of the shear band grains quite well as shown in Figure 3b.

Höppel et al. [2] reported the formation of shear bands in ultrafine-grained (UFG) copper of commercial purity. Like the micro shear bands discussed here for nickel, the shear bands in UFG copper consist of single layers of grains. However, there are remarkable differences: in the case of UFG copper the shear bands frequently intersect each other at less than 90° and consist of distinctly coarsened grains, which are not necessarily elliptical. In contrast, the micro shear bands considered here consist of elliptical grains (by definition) which are not much bigger than the rest, and only one system of micro shear bands is observed.

However, the mechanism responsible for the formation of micro shear bands is probably similar to that proposed by Mughrabi and Höppel [14]: the shear band formation starts at coarsened patches in the material and their growth is due to an interaction of cyclically induced grain coarsening and grain rotation, which both lead to a locally reduced strength of the material and, as a consequence, to a concentration of plastic deformation in the coarsened and/or rotated regions.

Obviously, here grain rotation plays the dominant role, leading to the pronounced shear texture observed. This is in accordance with observations of Hafok and Pippan [15] on high-pressure torsion (HPT)-deformed nickel where a square grid was introduced into the pre HPT sample ($\gamma = 64$, grain size $d = 400$ nm) before applying an additional shear of $\gamma = 1$. The post-shear evaluation of the grid indicates the formation of micro shear bands that cause local deformations of the microstructure. Based on their findings, Hafok and Pippan [15] exclude grain boundary sliding as the main deformation mechanism. Instead, they propose that intergranular slip of dislocations accounts completely for the observed microstructural features in post-shear-deformed HPT nickel. According to this, here both grain ellipticity and shear texture in the bands are most likely due to pronounced intergranular slip of dislocations.

Finally, based on the above findings it is reasonable to conclude that during cyclic deformation not only grain coarsening occurs from the beginning, but also the formation of micro shear bands. The increasing number and length of these bands, together with the ongoing grain coarsening, manifests as cyclic softening. At a certain point a local overlapping of evolving micro shear bands forms an easy glide path through the whole specimen volume where the plastic strain then localizes. The result is the apparently sudden formation of a macro shear band, which, in reality, is simply the termination of the formation and evolution of micro shear bands.

The authors gratefully acknowledge financial support of the Deutsche Forschungsgemeinschaft DFG, contract Sk 21/23-1. S.R.D and B.B. are grateful to the Alexander von Humboldt Foundation for their research fellowships.

[1] M.A. Meyers, A. Mishra, D.J. Benson, Progr. Mater. Sci. 51 (2006) 427–556.
[2] H.W. Höppel, C. Xu, M. Kautz, N. Barta-Schreiber, T.G. Langdon, H. Mughrabi, in: M. Zehetbauer, R.Z. Valiev (Eds.), Nanomaterials by Severe Plastic Deformation, Wiley-VCH, Weinheim, 2002, pp. 677–683.
[3] E. Thiele, C. Holste, R. Klemm, Z. Metallkd. 93 (2002) 730–736.
[4] L. Hollang, E. Hieckmann, C. Holste, W. Skrotzki, Mater. Sci. Eng. A 483 (2008) 406–409.
[5] M.K. Wong, W.P. Kao, J.T. Lui, C.P. Chang, P.W. Kao, Acta Mater. 55 (2007) 715–725.
[6] H. Mughrabi, H.W. Höppel, Inter. J. Fatigue 32 (2010) 1413–1427.
[7] S. Malekjani, P.D. Hodgson, P. Cizek, T.B. Hilditch, Acta Mater. 59 (2011) 5358–5367.
[8] Q.J. Wang, Z.Z. Du, L. Luo, W. Wang, J. Alloys Compd. (2012) 39–44.
[9] S.R. Dey, L. Hollang, B. Beausir, E. Hieckmann, W. Skrotzki, Scripta Mater. 62 (2010) 770–773.
[10] B. Beausir, J.J. Fundenberger, Software for Orientation Image Mapping, <http://benoitbeausir.free.fr>.

[11] G.R. Canova, U.F. Kocks, J.J. Jonas, Acta Metall. 32 (1984) 211–226.
[12] Z.F. Zhang, J. Eckert, L. Schultz, Acta Mater. 51 (2003) 1167–1179.
[13] W. Skrotzki, N. Scheerbaum, C.-G. Oertel, R. Arruffat-Massion, S. Suwas, L.S. Tóth, Acta Mater. 55 (2007) 2013–2024.
[14] H. Mughrabi, H.W. Höppel, in: D. Farkas, H. Kung, M. Mayo, H.V. Swygenhoven, J. Weertman (Eds.), MRS Proc., vol. 634, Warrendale, PA, 2001, pp. B2.1.1–B2.1.12.
[15] M. Hafok, R. Pippan, Scripta Mater. 56 (2007) 757–760.